

The Combined Use of Simulation and Navigation to Demonstrate Hip Kinematics

By Robert L. Thornberry, M.D., and Andrew J. Hogan
Tallahassee Orthopedic Clinic — Tallahassee, FL, USA

© 2009 The Journal of Bone and Joint Surgery, Inc. Reprinted from the Journal of Bone and Joint Surgery American, Volume 91, pp. 144-152 with permission.

Disclosure: The authors did not receive any outside funding or grants in support of their research for or preparation of this work. One or more of the authors, or a member of his or her immediate family, received, in any one year, payments or other benefits in excess of \$10,000 or a commitment or agreement to provide such benefits from a commercial entity (Smith and Nephew). No commercial entity paid or directed, or agreed to pay or direct, any benefits to any research fund, foundation, division, center, clinical practice, or other charitable or nonprofit organization with which the authors, or a member of their immediate families, are affiliated or associated.

Abstract

Computer navigation of total hip arthroplasty and computer simulation of hip motions based on collision detection were both introduced more than ten years ago. Neither of these promising technologies has achieved its full potential to improve patient outcomes. Combining these two technologies allows the individual strengths of each to more easily demonstrate hip kinematics in a clinically useful way. All normal and pathologic combined hip motions must be clearly and accurately reported to fully evaluate the kinematics involved in total hip arthroplasty, femoroacetabular impingement syndrome, and other hip disorders. The use of three-dimensional data graphs allows for a rapid and thorough evaluation of the very large data sets that are required for the purpose of making a complete report of all combined hip motions. Data can be obtained from simulations made with use of high-resolution computed tomographic scans and computer-aided implant-design files or from clinically obtained motion analysis on fresh cadavers or normal subjects. The use of these methods and graphics allows for the thorough evaluation of the geometries of current implant designs and will help improve future implant designs. The pathologic structures in hips with femoroacetabular impingement can be modeled in three dimensions, and surgical treatment plans can be developed to provide impingement-free normal hip motion without excessive osseous resection. The combination of these technologies provides hope for the improved surgical placement of total hip implants by providing the basis for a kinematic, impingement-based total hip navigation system.

Introduction

In 1996 and 1998, at the Annual Meetings of the American Academy of Orthopaedic Surgeons (AAOS), scientific exhibits were presented on hip navigation, hip range-of-motion simulations, and small-incision total hip arthroplasty¹⁻⁴. Each of these subjects has had an interesting history and development over the last ten years. Small-incision surgery exploded onto the scene and became both commonplace and controver-

sial^{5,6}. As a promising technology, hip navigation had a surge in exposure, if not popularity, but it has not been widely accepted in the United States^{7,8}. The combination of minimally invasive surgery and computer-assisted orthopaedic surgery spawned a series of courses around the globe during the last decade.

During this time, hip range-of-motion simulations were used primarily as marketing tools by industry to drive implant sales⁹, and their use as a research tool was limited¹⁰⁻¹². The fusion of navigation and simulation technologies has the potential to improve the understanding of normal and abnormal kinematics of the hip as well as the process capability (Six Sigma) of total hip arthroplasty. The recent identification of femoroacetabular impingement syndrome and its relationship to the etiology of hip arthritis underscores the need for more thorough and exacting methods to evaluate hip kinematics¹³.

Materials and Methods

HipNav, a validated computed tomography-based computer navigation and simulation program, was used to model hip motions from computed tomographic images of normal hips¹⁴. These hips represented an anonymous set of thirty-nine normal hip scans that were acquired at the New England Baptist Hospital¹⁵; in addition, ten normal hips (two hips from each of five cadavers) came from a cadaver laboratory. All computed tomographic scans were carefully screened to exclude hips with arthritis, femoroacetabular impingement, and hip dysplasia. Simulations of all available combined hip motions were calculated after the hips were carefully segmented to allow manipulation of the solid virtual femora and pelvis created in the software motion simulation program.

It was necessary to remove the femoral head in the simulations to ensure that no intra-articular impingements occurred due to the normal out-of-round variability of head and acetabular geometry. The soft tissues (labrum and capsule) about the hip were considered, and, on the basis of observations made by Tannast et al.¹⁵, five degrees were subtracted from hip motions based on collision detection of the bone models. These simulations created the normal data files of hip motion based on computed tomography (Fig. 1). Hip scans of patients with femoroacetabular impingement were compared with these normal scans.

The same process was utilized for the modeling of total hip motions. A single computed tomographic model was used to place a total hip computer-assisted design model (stereolithography format) in multiple different orientations with multiple implant types and head sizes. Data were recorded for all

The Combined Use of Simulation and Navigation to Demonstrate Hip Kinematics

(continued)

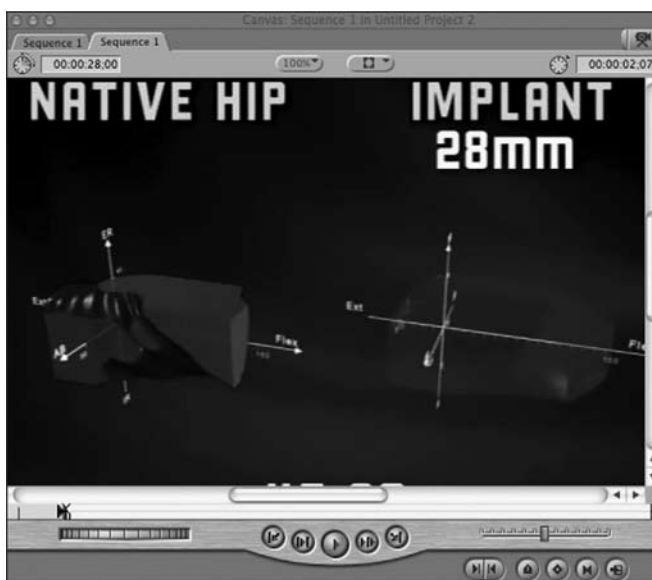


Figure 1: Data graph of computed tomography-based hip motions of a normal hip (red) and the implant motions graph of a 28-mm total hip prosthesis (blue). ER = external rotation; Ext = extension; Flex = flexion; IR = internal rotation; and AB = abduction.

implant-on-implant impingement and nonimpingement points. The nonimpingement points were then selected for further study. Each data set included one to two million data points. Specialized add-on software was written to allow HipNav to run sequential simulations in multiple positions, allowing all potential positions to be modeled.

In order to accurately present all of the data in a single graph, it was necessary to use a three-dimensional data graph or point cloud graph (Fig. 1). By convention, the six motions of the hip were assigned positive or negative values in the Cartesian coordinate system. Flexion was positive and extension negative on the y-axis; abduction was positive and adduction negative on the x-axis; and external rotation was positive and internal rotation negative on the z-axis (Table I). A custom filtering program was written that identified the outer boundary of the three-dimensional data graph, which was required to reduce the number of data points to a manageable number, allowing manipulation of the data graphs.

TABLE I Definition of Range of Motion Parameters and Axes*

Motion	X-Axis		Y-Axis		Z-Axis	
	AB(1) (1 /-) (deg)	AD (-) (deg)	Flex (1) (deg)	Ext (-) (deg)	ER (1) (deg)	IR (-) (deg)
Maximum	65 (50)	50 (25)	150	45	65 (45)	45

*Numbers in parentheses are range-of-motion parameters reported in the literature.²⁰⁻²⁶

AB= abduction; AD = adduction; Flex = flexion; Ext = extension; ER = external rotation; and IR = internal rotation.

All files were reported as script files, which could cross computer platforms. The original script files from HipNav were created in Linux Red Hat (Red Hat, Raleigh, North Carolina), then transferred to a Windows XP computer for statistical modeling with use of Maple V Release 5.1 (Waterloo Maple, Waterloo, Ontario, Canada). The Maple graphs lacked clarity for presentation purposes and were modeled in three-dimensional Studio MAX Autodesk 3ds Max software (Autodesk, San Rafael, California) and Adobe After Effects 7.0 software (Adobe Systems, San Jose, California). Very vivid, high-resolution renderings could then be produced, allowing for clear and unambiguous representation and interpretation.

The data collected on normal cadaver hip motions were obtained by means of one of us (R.L.T.) manually moving a normal fresh cadaver hip through a range of motion and by means of reference arrays attached to the femur and pelvis with use of modified BrainLAB VectorVision (BrainLAB, Westchester, Illinois) software. All osseous landmarks were fully exposed, and small screws were placed to reduce registration errors. All hips were evaluated for arthritis, femoroacetabular impingement, and hip dysplasia with use of computed tomographic scans or through exposure by dissection.

VectorVision software reported ten data points of the hip position per second relative to the pelvic plane. With use of the same convention, three-dimensional graphs were created with use of the Maple software. It usually took about twenty minutes of continuous movement to obtain sufficient data points to generate a reasonable graph. The graphs then required the application of a wrap-type program for the purpose of surrounding the collected points to provide a solid three-dimensional graph. These graphs represented all of the possible positions in which each cadaveric hip could be placed (Fig. 2-A). More than forty normal cadaveric hips have been studied to date for the creation of a database of normal hip motion.

Simulations were run for different head sizes, implants, implant positions, liners (lipped compared with nonlipped), and lipped liner positions. Results were graphed in Maple and evaluated by overlaying one graph on another. When a simulation graph demonstrated an important point or insight, a three-dimensional Studio MAX animation was made.

Results

Multiple studies have been reported in which these techniques have been used¹⁶⁻¹⁹. The combined-motions graphs that were obtained with use of HipNav show a much more complex picture of hip range of motion than previously described (Table II). This method is of particular importance in the evaluation of femoroacetabular impingement. The ability to graphically represent the loss of motion and the areas that need to be altered surgically can be a powerful tool in the treatment of this disorder.

The cadaveric hip range of motion was far greater than what was expected or had been previously reported (Fig. 2-B)²⁰⁻²⁶. This necessitated increasing the parameters for the

The Combined Use of Simulation and Navigation to Demonstrate Hip Kinematics

(continued)

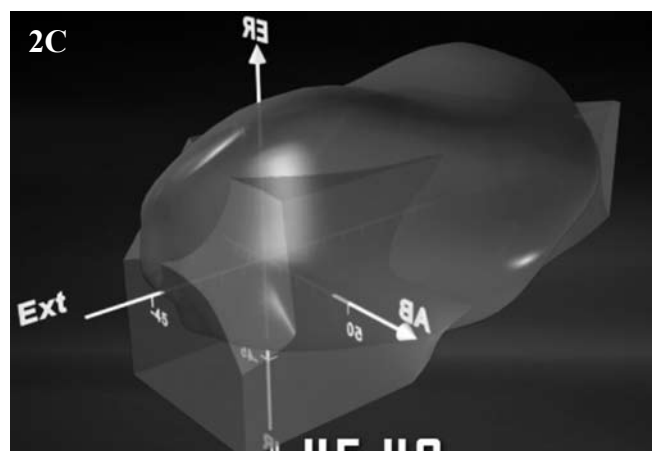
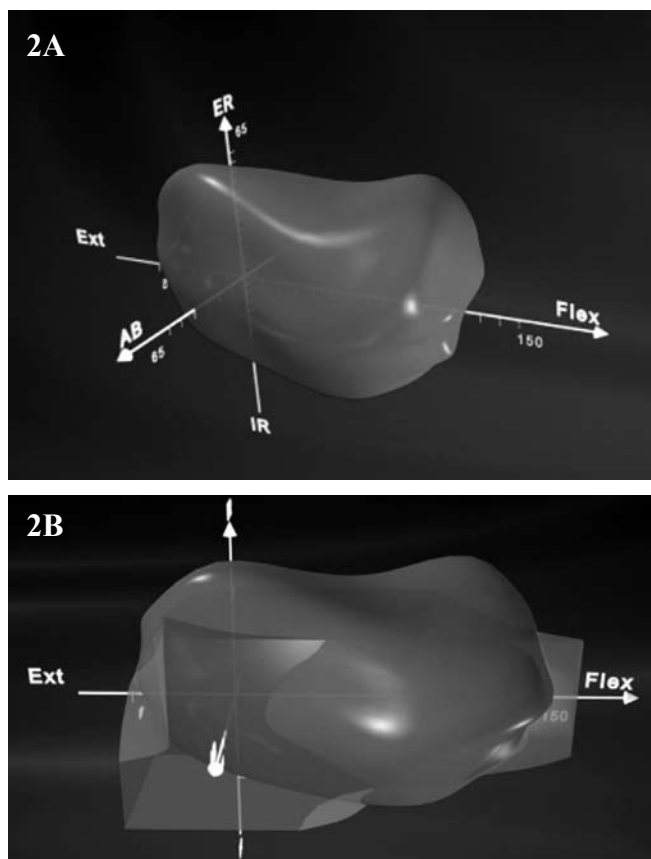


Figure 2-A: Normal, cadaveric combined-motions graph on a standard Cartesian coordinate system. ER = external rotation; Ext = extension; Flex = flexion; and IR = internal rotation. **Figure 2-B:** Normal, cadaveric combined-motions graph demonstrating the need for expanded hip-motion parameters. Red = normal cadaveric range of motion; and blue = clinically based range of motion parameters as reported in the literature. Ext = extension; and Flex = flexion. **Figure 2-C:** Alternate view of the necessity for an expansion of hip-motion parameters for accurate cadaveric combined-motions graphs. Red = normal cadaveric range of motion; and blue = clinically based range-of-motion parameters as reported in the literature. Ext = extension; ER = external rotation; IR = internal rotation; and AB = abduction.

three-dimensional data graphs that were used to model the motions of hip implants (Fig. 2-C). The charted cadaveric hip motions were most closely aligned with the simulated motions reported in the work of Sugano et al.²⁴ than with the motions in any of the previous clinical works found in the literature (Table II).

Ten cadaveric hips, with both computed tomographic and cadaveric motions recorded, showed similarities. However, the complex nature of the hip capsular ligaments restricted certain hip motions, in addition to osseous impingement, in many movements. Graphic analyses were most similar during combined flexion and internal rotation. These combined motions

TABLE II Hip Range of Motion as Reported in the Literature*

Authors (Year)	Extension (deg)	Flexion (deg)	Abduction (deg)	Adduction (deg)	Internal Rotation (deg)	External Rotation (deg)
Ahlberg et al. ²¹ (1988) †	13.9 ± 5.5	130.8 ± 14.0	50.8 ± 6.1	30.1 ± 6.5	36.7 ± 12.2	72.9 ± 10.7
Roaas and Andersson ²⁶ (1982) †	9.5 ± 5.3	120.4 ± 8.3	38.6 ± 7.2	30.5 ± 7.3	32.6 ± 8.2	33.7 ± 6.8
Boone and Azen ²⁵ (1979) †	9.8 ± 6.8	122.3 ± 6.1	45.9 ± 9.3	26.9 ± 4.1	47.3 ± 6.0	47.2 ± 6.3
AAOS ²⁷ (1965)	28	113	48	31	45	45
AAOS ³⁰ (1994)	30	120	NA	NA	NA	NA
Japanese Orthopaedic Association ²³ (1995)	15	125	NA	NA	NA	NA
Sugano et al. ²⁴ (women) (2003)	55.5	127.4	34	64.4	NA	40.7
Sugano et al. ²⁴ (men) (2003)	67.4	117.4	37	59.7	NA	47.9

*AAOS= American Academy of Orthopaedic Surgeons. NA = not available. †Range of motion reported as degrees ± standard deviation.

The Combined Use of Simulation and Navigation to Demonstrate Hip Kinematics

(continued)

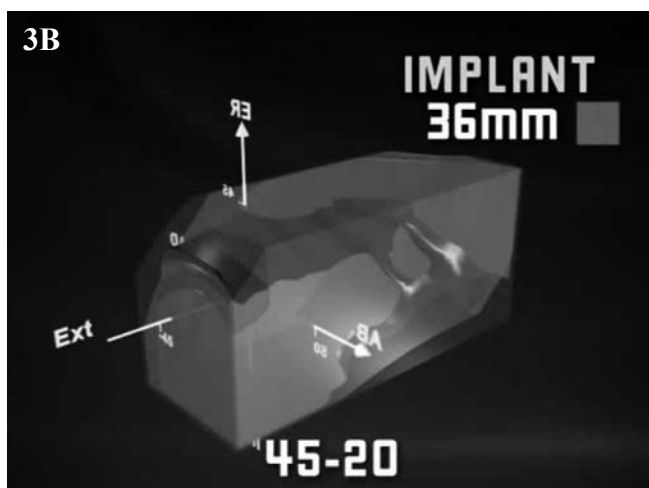
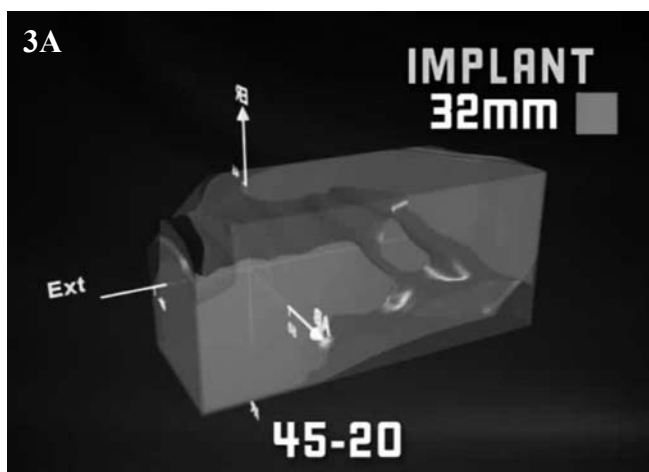


Figure 3-A: Increase in available range of motion with a 32-mm head size. Red = native hip computed tomography-based range of motion; blue = range of motion from 28-mm head size; and orange = range of motion from 32-mm head size. Ext = extension; ER = external rotation; and AB = abduction. **Figure 3-B:** Additional increases in available range of motion achieved with a 36-mm head size, as compared with a 32-mm head size. Red = native hip computed tomography-based range of motion; blue = range of motion from 28-mm head size; and green = range of motion from 32-mm head size. Ext = extension; ER = external rotation; and AB = abduction.

appear to be more related to osseous impingement than to ligament restraint.

Whether computed tomographic or cadaveric-determined range-of-motion standards were used, normal hip motion could not be restored with a 28-mm head prosthesis, regardless of the cup orientation. If a lipped liner was used, the range of motion dropped even more precipitously. Range of motion continued to improve with use of a 32-mm head (Fig. 3-A), and even more with use of a 36-mm head (Fig. 3-B). The available motion of the 36-mm head was acceptable at 45 of abduction and 35 of combined anteversion, but accurate placement was still necessary to avoid loss of the normal motions as was seen in the cadaver studies.

Non-navigated placement of a hip implant, as reported in the literature, is quite variable when computed tomographic scans are used to measure placement²⁷. The accuracy of implantation that is needed to ensure the restoration of normal range of motion of the hip is much more exacting than the accuracies that have been reported with non-navigated techniques²⁷. Simulations were performed of multiple combined anteversion and abduction angles. These data were then animated with constant abduction (Figs. 4-A and 4-B) and constant anteversion (Figs. 4-C and 4-D) of the cup.

The impingement proved greatest when the acetabulum was over-anteverted, with impingement occurring in extension and external rotation (Fig. 4-A)²⁸. Placing the cup in a more vertical orientation decreases the prevalence of impingement but also increases the stresses to the bearing surfaces and decreases the “jumping distance” for dislocation. Newer, hard-on-hard bearing surfaces do not tolerate vertical cup placement. It has been suggested that cups should be placed more horizontally. This horizontal positioning increases impingement in both flexion and extension (Fig. 4-C).

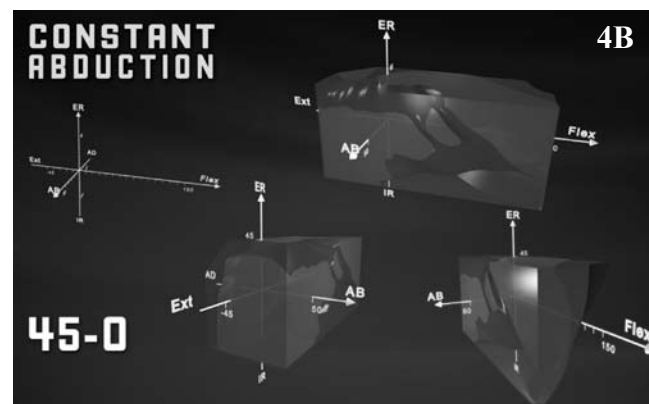
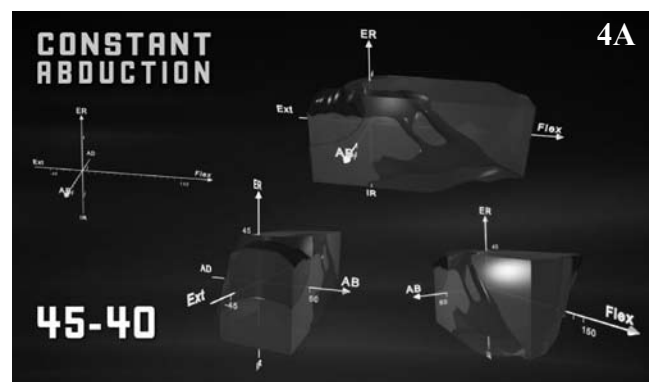


Figure 4-A: Combined-motions graphs of an over-anteverted acetabular cup. Red = native hip computed tomography-based range of motion; and blue = range of motion from 28-mm head size. ER = external rotation; IR = internal rotation; Ext = extension; Flex = flexion; AB = abduction; and AD = adduction. **Figure 4-B:** Combined-motions graphs of an under-anteverted acetabular cup. Red = native hip computed tomography-based range of motion; and blue = range of motion from 28-mm head size. ER = external rotation; IR = internal rotation; Ext = extension; Flex = flexion; AB = abduction; and AD = adduction.

The Combined Use of Simulation and Navigation to Demonstrate Hip Kinematics

(continued)

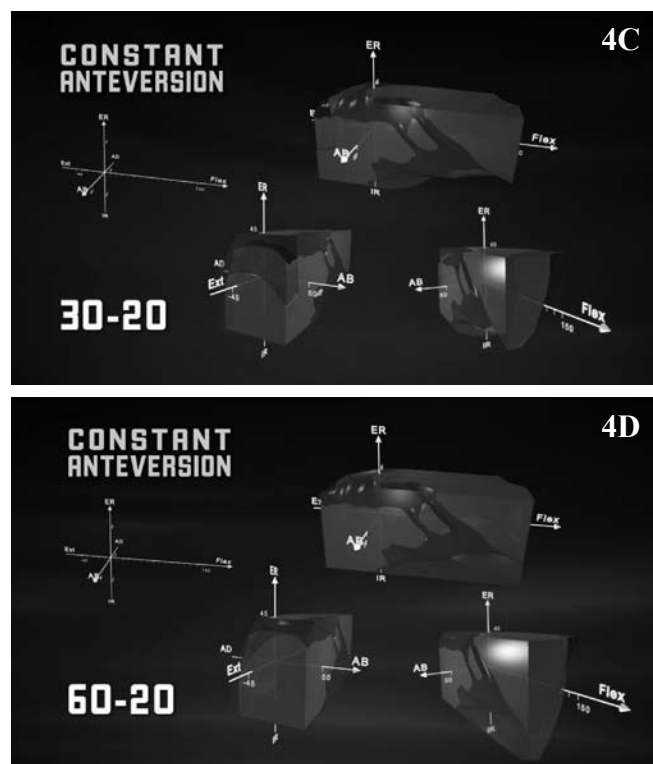
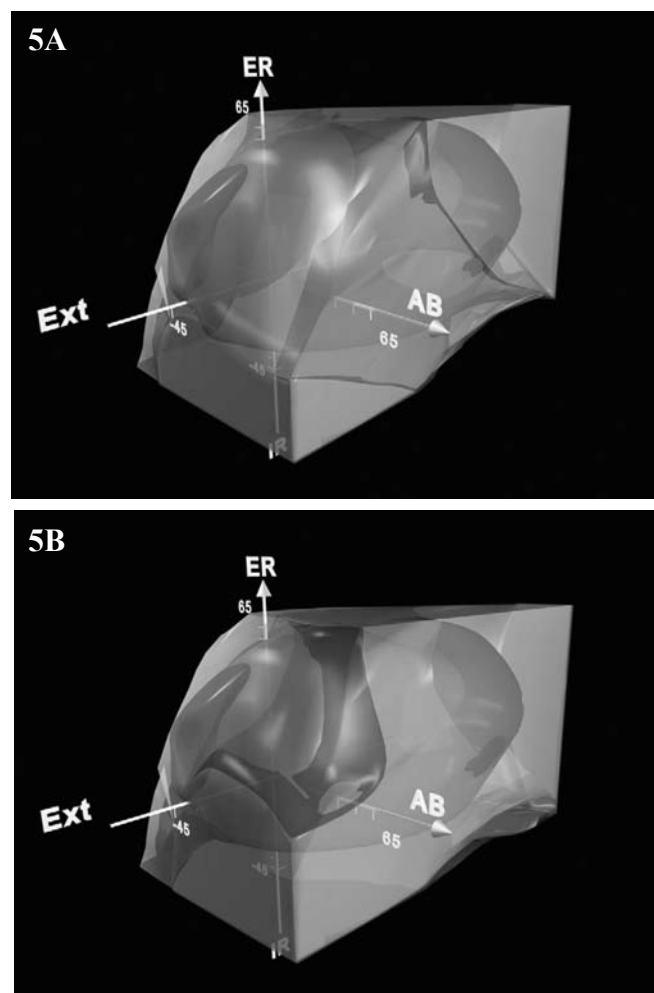


Figure 4-C: Combined-motions graphs of a horizontally positioned acetabular cup. Red = native hip computed tomography-based range of motion; and blue = range of motion from 28-mm head size. ER = external rotation; IR = internal rotation; Ext = extension; Flex = flexion; AB = abduction; and AD = adduction. **Figure 4-D:** Combined-motions graphs of a vertically positioned acetabular cup. Red = native hip computed tomography-based range of motion; and blue = range of motion from 28-mm head size. ER = external rotation; IR = internal rotation; Ext = extension; Flex = flexion; AB = abduction; and AD = adduction.

Augmented liners, which have been shown to decrease dislocation, are frequently used²⁹. In certain positions, loss of motion to impingement can be anticipated, although the prevalence of dislocation may decrease. It has previously been suggested that the proper placement of the augmented liner is at the four o'clock position³⁰. Simulations were performed to evaluate augmentation placement and the effect on available range of motion on the basis of the cadaveric range-of-motion data. The simulations did not indicate any significant decrease in impingement by lowering the center of augmentation to the four o'clock position from the one o'clock or three o'clock position (Fig. 5-A). Substantial decreases in impingement did not occur until the six o'clock position (Fig. 5-B). A 20 augmented liner, specifically optimized to limit impingement and placed directly posterior, caused a decrease in motion to impingement in external rotation and extension that was equivalent to over-anteverting the acetabular cup by 30. A poorly designed liner or femoral neck geometry would have fared even worse³¹.

The most promising application of the combined use of navigation and simulation has been the development of a new navigation system based on the forced impingement of



Figures 5-A and 5-B: Placement of the hooded liner in the three o'clock position (Fig. 5-A) and six o'clock position (Fig. 5-B) in the left hip. Red = native hip cadaveric range of motion; and orange = additional impingement from hooded insert. ER = external rotation; IR = internal rotation; AB = abduction; and Ext = extension.

the trial hip with a “gizmo” neck augmentation device (Fig. 6-A). This creates a signature three-dimensional graph or three dimensional fingerprint (appearing like a funnel cake or tube) of collision detection points that allows for the solution of the relative position of the acetabular implant without registration of the pelvic plane (Fig. 6-B). Every possible position must be simulated to create a data set that is used to identify the cup-stem orientation. Every “tube” graph is related to an implant graph that identifies the available hip motions in each implant orientation (Fig. 6-C). By overlaying these data on the normal hip motions, optimal results can be obtained (Fig. 6-D). This method requires thousands of simulations and several terabytes of data-filtering to create a database.

These virtual simulations do not need to allow for the point acquisition errors and repositioning that have limited the accuracy and usefulness of computed tomography-free navigation, and thus there is a potential for substantial improvements in the efficiency and accuracy of hip navigation.

The Combined Use of Simulation and Navigation to Demonstrate Hip Kinematics

(continued)

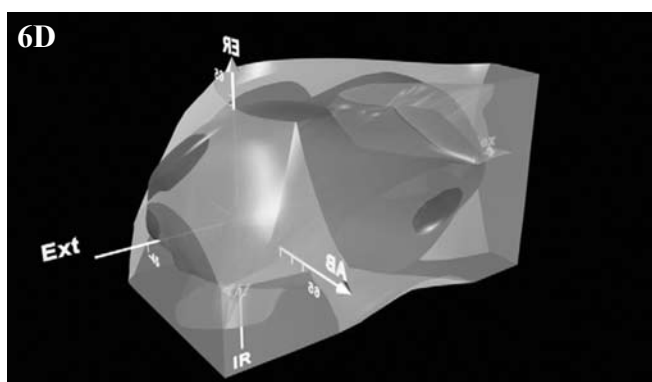
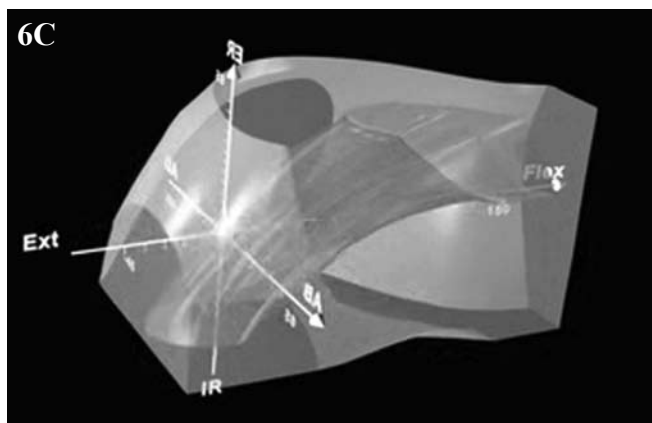
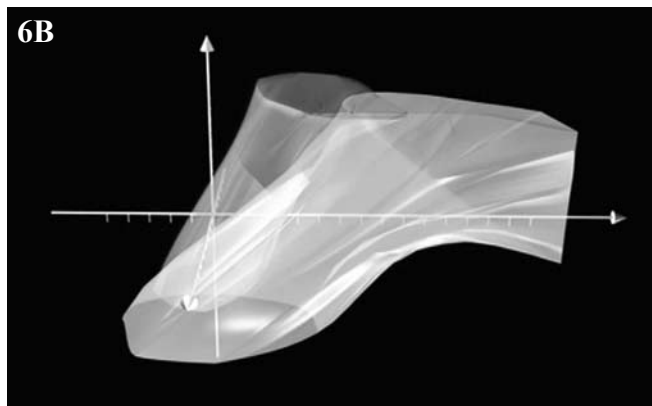
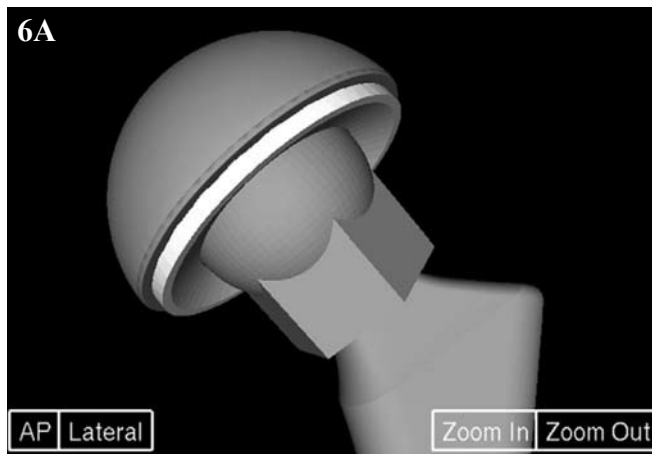


Figure 6-A: Computer-generated, three-dimensional model of the “gizmo” neck augmentation device. **Figure 6-B:** 60 abduction, 20 anteversion (green) and 30 abduction, 20 anteversion (yellow) tube graphs demonstrating difference in shape. **Figure 6-C:** Total hip combined-motions graph (yellow) with corresponding gizmo tube graph (blue). ER = external rotation; IR = internal rotation; Ext = extension; Flex = flexion; AB = abduction; and AD = adduction. **Figure 6-D:** Combined graph of combined hip implant motions (yellow), gizmo tube graph (blue), and cadaveric combined motions (red) for a 28-mm head in ideal position (45 abduction and 35 combined anteversion). Ext = extension; ER = external rotation; IR = internal rotation; and AB = abduction.

Multiple positions were modeled, both with and without the gizmo device, and graphs were obtained. The subtle differences, even by only one degree, of the tube or gizmo graphs are variable enough to allow for clear differentiation of obtained and simulated data.

Discussion

The ability to view all combined hip motions in a single graph is a great advantage in the evaluation of hip kinematics. It takes some time to become comfortable with the three-dimensional graphic technique and to understand the differences displayed when overlaying one graph on another. The methodology supports the use of data, from any source and in all computer platforms, that can be displayed relative to the pelvic plane in script files.

Recent studies have suggested that the pelvic tilt is critical for correct cup placement³². The cadaveric data to date reveal that the range of motion of the hip relative to the pelvic plane in fresh cadavers is quite consistent. Variability of the tilt may be especially important in radiographic measurements and non-navigated cup positioning, but it had no noticeable effect on the maximal normal motions that were measured relative to the pelvic plane in the cadavers that were studied.

The lack of motion due to impingement that was clearly demonstrated by 28-mm heads is a cause for concern. Small acetabular components limit the size of the femoral head that can be used. Larger bearings have clearly been shown to increase the amount of hip motion possible before impingement occurs (Figs. 3-A and 3-B)^{33,34}. The use of larger femoral heads did not obviate the need for accuracy in implant placement, and the simulations indicate that both an improved geometry with larger head sizes and an improved accuracy are needed to improve the process capability of total hip arthroplasty.

With use of these methods, a standard of minimal total hip implant motion can and should be determined. Sixty percent of retrieved cups in one study demonstrated signs of impingement³⁵, half with moderate to severe damage. This resulted in a doubling of polyethylene wear in the hips with moderate to severe damage. The poor motion provided by some earlier modular total hip arthroplasty designs needs to be fully documented, exposed, and corrected. This methodology can calculate the anticipated rate of implant-on-implant impingement of any prosthesis, knowing the implant geometry and a

The Combined Use of Simulation and Navigation to Demonstrate Hip Kinematics

(continued)

given surgeon's implantation variability. This information can determine if total hip arthroplasty navigation, although not in popular use today, may be necessary to achieve adequate post-operative range of motion of the hip.

If the implant selected can achieve acceptable combined motions without impingement, despite the wide range of expected variability of surgical implantation, it should be documented. However, if certain implant geometries cannot provide acceptable motion within the limits of variability of surgical implantation, they should either not be made available or should carry a disclaimer stating that the implant is not recommended for use without the accompanying use of navigation or an increased femoral head size.

A higher prevalence of dislocation with certain implant designs has been reported³¹. In addition, certain designs have been shown to have increased impingement at the time of retrieval analysis³⁶.

With respect to limitations, the techniques and concepts reported are forward-looking and a commercially available working system is not yet available; when such a system is introduced, it will likely include further improvements and enhancements. At present, this remains a work in progress. Additional studies on normal subjects and more cadavers must be done to create a statistically valid normal hip-motion database. Statistical techniques for determining the means and standard deviations of the three-dimensional data graphs have not been completed. Although intuitively reasonable, a working kinematic navigation method has yet to be validated to decrease the prevalence of dislocation and impingement.

Future Developments

The combined use of computer simulation and computer navigation of the hip is a fertile field for study and offers the possibility for improvement in implant design, hip navigation systems, and the treatment of femoroacetabular impingement syndrome. Future computer tools will soon be available that will more accurately diagnose and surgically treat femoroacetabular impingement. Improved total hip arthroplasty implant designs will result in fewer impingements and dislocations.

Future use of a new method of evaluating intraoperative implant positions with use of three-dimensional data graphs is suggested. Graphs of a patient's normal expected hip motions (from a navigation-obtained database), the available hip motions from the implant, and the intraoperatively obtained tube graphs can together confirm intraoperatively that the patient will have satisfactory impingement-free range of motion of the hip postoperatively.

References

1. Thornberry RL, Lavernia CJ, Barrack RL, Tozakoglou E. The effects of neck geometry and acetabular design on the motion to impingement in total hip reconstruction (THR). Presented at the 65th Annual Meeting of the American Academy of Orthopaedic Surgeons; 1998 Mar 19-23; New Orleans, LA. SE 046.
2. Lavernia CJ, Barrack RL, Thornberry RL, Tozakoglou E. The effects component position in motion to impingement and dislocation in total hip reconstruction (THR). Presented at the 65th Annual Meeting of the American Academy of Orthopaedic Surgeons; 1998 Mar 19-23; New Orleans, LA. SE 058.
3. DiGioia AM 3rd, O'Toole RV, Jaramaz B, Simon D, Blackwell M, Morgan F. A computer-assisted planner and intraoperative guidance system for the accurate placement of acetabular implants. Presented at the 63rd Annual Meeting of the American Academy of Orthopaedic Surgeons; 1996 Feb 22-26; Atlanta, GA. SE 075.
4. Crockett HC, Wright JM, Sculco TP, Bates J. Mini-incision for primary total hip arthroplasty. Presented at the 65th Annual Meeting of the American Academy of Orthopaedic Surgeons; 1998 Mar 19-23; New Orleans, LA. SE 060.
5. Berry DJ. "Minimally invasive" total hip arthroplasty. *J Bone Joint Surg Am.* 2005; 87:699-700.
6. Berger RA, Jacobs JJ, Meneghini RM, Della Valle C, Paprosky W, Rosenberg AG. Rapid rehabilitation and recovery with minimally invasive total hip arthroplasty. *Clin Orthop Relat Res.* 2004;429:239-47.
7. Haaker RG, Tiedjen K, Ottersbach A, Rubenthaler F, Stockheim M, Stiehl JB. Comparison of conventional versus computer-navigated acetabular component insertion. *J Arthroplasty.* 2007;22:151-9.
8. DiGioia AM 3rd, Jaramaz B, Plakseychuk AY, Moody JE Jr, Nikou C, Labarca RS, Levison TJ, Picard F. Comparison of a mechanical acetabular alignment guide with computer placement of the socket. *J Arthroplasty.* 2002;17:359-64.
9. Paradigm Productions. Hip range of motion comparisons. CD-ROM. Memphis, TN: Smith and Nephew; 1998.
10. Noble PC, Sugano N, Johnston JD, Thompson MT, Conditt MA, Engh CA Sr, Mathis KB. Computer simulation: how can it help the surgeon optimize implant position? *Clin Orthop Relat Res.* 2003;417:242-52.
11. Otake Y, Suzuki N, Hattori A, Hagio K, Sugano N, Yonenobu K, Ochi T. Four dimensional model of the lower extremity after total hip arthroplasty. *J Biomech.* 2005;38:2397-405.
12. Leardini A, Belvedere C, Astolfi L, Fantozzi S, Viceconti M, Taddei F, Ensi A, Benedetti MG, Catani F. A new software tool for 3D motion analyses of the musculoskeletal system. *Clin Biomech (Bristol, Avon).* 2006;21:870-9.
13. Ganz R, Parvizi J, Beck M, Leunig M, N'otzli H, Siebenrock KA. Femoroacetabular impingement: a cause for osteoarthritis of the hip. *Clin Orthop Relat Res.* 2003;417:112-20.
14. Eckman K, Nikou C, Lattanzi R, Jaramaz B, DiGioia AM 3rd. Experimental validation of hip range of motion simulator. Presented at the 3rd Annual Meeting of the International Society for Computer Assisted Orthopaedic Surgery; 2003 Jun 18- 21; Marbella, Spain. Special poster no. 17.
15. Tannast M, Kubiak-Langer M, Langlotz F, Puls M, Murphy SB, Siebenrock KA. Non-invasive three-dimensional assessment of femoroacetabular impingement. *J Orthop Res.* 2007;25:122-31.
16. Thornberry RL, Nelson LS. CT evaluation of combined native hip ROM using computer simulations. Presented at the 6th Combined Meeting of the Orthopaedic Research Societies; 2007 Oct 21-24; Honolulu, HI. Poster no. 0459.
17. Thornberry RL, Nelson LS. Combined native hip range of motions. Presented at the 6th Combined Meeting of the Orthopaedic Research Societies; 2007 Oct 21- 24; Honolulu, HI. Poster no. 0456.
18. Thornberry RL, Nelson LS. Effect of elevated-rim liner position on motion to impingement in THA. Presented at the 54th Annual Meeting of the Orthopaedic Research Society; 2008 Mar 2-5; San Francisco, CA. Poster no. 1761.
19. Thornberry RL, Nelson LS. Effect of femoral head size and implantation variability on reestablishing normal combined hip motions. Presented at the 6th Combined Meeting of the Orthopaedic Research Societies; 2007 Oct 21-24; Honolulu, HI. Poster no. 0159.
20. Green WBB, Heckman JD, editors. The clinical measurement of joint motion. Rosemont, IL: American Academy of Orthopaedic Surgeons; 1994. The hip; p 99-114.
21. Ahlberg A, Moussa M, Al-Nahdi M. On geographical variations in the normal range of joint motion. *Clin Orthop Relat Res.* 1988;234:229-31.
22. Joint motion: method of measuring and recording. Chicago: American Academy of Orthopaedic Surgeons; 1965.
23. Range of joint motion and method of measurement. Tokyo: Japanese Orthopaedic Association; 1995.
24. Sugano N, Yamanashi W, Sasama T, Sato Y, Nishii T, Miki H, Yoshikawa H. Ranges of motion in anatomically normal hips using computer collision detection. Read at the 49th Annual Meeting of the Orthopaedic Research Society; 2003 Feb 2-5; New Orleans, LA. Paper no. 0155.
25. Boone DC, Azen SP. Normal range of motion of joints in male subjects. *J Bone Joint Surg Am.* 1979;61:756-9.
26. Roaas A, Andersson GB. Normal range of motion of the hip, knee and ankle joints in male subjects, 30-40 years of age. *Acta Orthop Scand.* 1982;53:205-8.
27. Minoda Y, Kadawaki T, Kim M. Acetabular component orientation in 834 total hip arthroplasties using a manual technique. *Clin Orthop Relat Res.* 2006;445:186-91.
28. Yamaguchi M, Akisue T, Bauer TW, Hashimoto Y. The spatial location of impingement in total hip arthroplasty. *J Arthroplasty.* 2000;15:305-13.
29. Cobb TK, Morrey BF, Ilstrup DM. The elevated-rim acetabular liner in total hip arthroplasty: relationship to postoperative dislocation. *J Bone Joint Surg Am.* 1996;78:80-6.
30. Malik A, Maheshwari A, Dorr LD. Impingement with total hip replacement. *J Bone Joint Surg Am.* 2007;89:1832-42.
31. Barrack RL. Dislocation after total hip arthroplasty: implant design and orientation. *J Am Acad Orthop Surg.* 2003;11:89-99.
32. Babisch JW, Layher F, Amiot LP. The rationale for tilt-adjusted acetabular cup navigation. *J Bone Joint Surg Am.* 2008;90:357-65.
33. Crowninshield RD, Maloney WJ, Wentz DH, Humphrey SM, Blanchard CR. Biomechanics of large femoral heads: what they do and don't do. *Clin Orthop Relat Res.* 2004;429:102-7.
34. Burroughs BR, Hallstrom B, Golladay GJ, Hoeffel D, Harris WH. Range of motion and stability in total hip arthroplasty with 28-, 32-, 38-, and 44-mm femoral head sizes. *J Arthroplasty.* 2005;20:11-9.
35. Usrey MM, Noble PC, Rudner LJ, Conditt MA, Birman MV, Santore RF, Mathis KB. Does neck/liner impingement increase wear of ultrahigh-molecular-weight polyethylene liners? *J Arthroplasty.* 2006;21(6 Suppl 2):65-71.
36. Yamaguchi M, Bauer TW, Hashimoto Y. Three-dimensional analysis of multiple wear vectors in retrieved acetabular cups. *J Bone Joint Surg Am.* 1997;79: 1539-44.